

Carnot's theorem as Noether's theorem for thermoacoustic engines

Eric Smith

*Los Alamos National Laboratory, Earth and Environmental Sciences Division, Los Alamos, New Mexico 87545
and Applied Research Laboratories, The University of Texas at Austin, Austin, Texas 78713-8029*

(Received 30 March 1998)

Onset in thermoacoustic engines, the transition to spontaneous self-generation of oscillations, is studied here as both a dynamical critical transition and a limiting heat engine behavior. The critical transition is interesting because it occurs for both dissipative and conservative systems, with common scaling properties. When conservative, the stable oscillations above the critical point also implement a reversible engine cycle satisfying Carnot's theorem, a universal conservation law for entropy flux. While criticality in equilibrium systems is naturally associated with symmetries and universal conservation laws, these are usually exploited with global minimization principles, which dynamical critical systems may not have if dissipation is essential to their criticality. Acoustic heat engines furnish an example connecting equilibrium methods with dynamical and possibly even dissipative critical transitions: A reversible engine is shown to map, by a change of variables, to an equivalent system in apparent thermal equilibrium; a Noether symmetry in the equilibrium field theory implies Carnot's theorem for the engine. Under the same association, onset is shown to be a process of spontaneous symmetry breaking and the scaling of the quality factor predicted for both the reversible *and irreversible* engines is shown to arise from the Ginzburg-Landau description of the broken phase. [S1063-651X(98)00209-8]

PACS number(s): 05.70.Jk, 43.35.+d, 43.20.+g

I. INTRODUCTION: THERMOACOUSTIC ONSET AS A CRITICAL TRANSITION

The local gas dynamics and mode stability of various thermoacoustic engines are subjects treated extensively, and in considerable quantitative detail, in the acoustics literature [1–10]. Many global engine properties, though, in particular the striking qualitative resemblance of the driven sound intensity to the order parameter in a classical critical transition, have not been considered at all. The critical interpretation of thermoacoustic onset is developed here because it exposes two relations between equilibrium and dynamical critical systems, which may have expressions as more general principles. The first is that reversibility, in some sense, is indistinguishable from equilibrium. The second is that Carnot's theorem, a thermodynamic transport relation for engines, may be viewed as a consequence of spontaneous symmetry breaking, describing a Noether current for the symmetry hidden by the critical transition.

Complete generality is not attempted in this derivation. Rather, the approach is to demonstrate these relations by a thorough analysis of a specific engine and then show in what respects it represents more general cases. Though no comparable, global treatment of the particular cycle considered here has been done before, enough of the results coincide with those in the standard thermoacoustics literature that straightforward aspects of the dynamical analysis are relegated to two appendixes, so the main text can focus on issues of criticality.

A. Heuristics

A simple thermoacoustic engine consists of a gas resonator, a stack of plates or matrix of pins (generically called a 'stack') in the flow stream of the gas to act as a regenerator,

and connections at the stack ends to hot and cold reservoirs [4]. The temperature difference between the reservoirs imposes a thermal gradient on the stack. For gradients below a critical value determined by properties of the gas and resonator, the gas is quiescent, the reservoirs exchange heat only by conduction, and any sound excited in the resonator decays exponentially. As the gradient approaches the critical value from below, the time constant for decay of the fundamental resonator mode diverges or, equivalently, the inverse of its quality factor goes to zero [5]. For driving gradients above the critical value, from quiescent initial conditions, oscillations of the lowest mode are spontaneously generated and initially grow exponentially, later slowing as the sound intensity approaches some saturation value. The (negative) inverse quality factor above the critical gradient describes the *growth* time constant and is the smooth continuation of the inverse quality function for decay, through the critical point [6]. If the driving gradient is reduced to critical from above, the saturation value of sound in the engine goes to zero with some steep slope [11].

This process corresponds heuristically to a classical phase transitions as follows: Statistical phonons in the resonator, though classical field excitations, are the "microscopic" degrees of freedom of the system. For thermal driving gradients below critical, their mean value is zero and time translation, which implies conservation of energy in the engine/reservoir system, is also (trivially) a symmetry of the classical sound background. Above the critical gradient, statistical phonons "freeze" into the coherent sound mode implementing the engine cycle. While time translation is still a continuous symmetry of the microscopic dynamics and energy in the engine/reservoir system is still conserved, this symmetry is not manifest in the excited mode, which is preserved only under discrete shifts by a multiple of the cycle period.

The intensity of excited sound at saturation thus serves as an order parameter and the temperature gradient along the thermoacoustic driving stack, appropriately nondimensionalized with the mean engine temperature and sound wavelength, is the effective coupling controlling the transition. The stable intensity in the running state has the nonanalytic dependence on the coupling (identically zero for gradients below critical, finite for gradients above) characteristic of equilibrium critical systems with spontaneously broken symmetry [12].

The symmetry broken by onset is time translation in the engine/reservoir system. Phase coherence of the working cycle has long-range order in time, consistent with the identification of the running engine state as its “frozen” state. From this correspondence, one would expect a thermoacoustic engine on the critical point to be characterized by phase-coherent episodes of running of all durations, with some scale-free (e.g., $1/f$) statistics. The running state near the critical point should display a weak coherent background, with superposed phase noise having a possibly universal distribution [13] (phase fluctuations being the Goldstone mode generated by local time translation of the coherent background).

No such nontrivial scaling properties of onset have been measured [14]. However, the inverse of the quality factor Q , a temporal coherence length in units of cycle period, has been studied for standing-wave engines *through* onset [5,6]. Measured $1/Q$ was linearly proportional to the driving gradient, in agreement with stack gain predictions. This classical scaling relation will be shown below to correspond to a mean-field prediction of Ginzburg-Landau theory and provides one indication that onset is critical.

B. Criticality and symmetry

In equilibrium systems, criticality is generally associated with spontaneous symmetry breaking [15] because such transitions create scale-free correlations at finite physical temperatures [16]. A corollary of this association, that critical systems have degenerate frozen backgrounds related by hidden symmetries, has profound implications, such as Goldstone's theorem [17]. However, whereas the symmetries of equilibrium critical systems can often be encoded in a classical Ginzburg-Landau free energy [18], dynamical critical processes are often intrinsically dissipative [19], so their governing equations cannot be obtained from the conservative sector of a classical action alone.

Acoustic heat engines are interesting in view of this dichotomy because versions exist with either intrinsically dissipative [3,4], or nonintrinsically dissipative cycles [7,8]. Onset is much the same at the level of the equations of motion in both cases, but as will be shown below, the nondissipative engine may be mapped by a change of field variables to an equilibrium system, described by a classical free energy, with a spontaneously broken symmetry and important associated conservation law.

The one universal relation satisfied by all reversible engines is Carnot's theorem [20]. It is shown here that, for the reversible (necessarily nondissipative) thermoacoustic cycle, Carnot's theorem is implied by a Noether symmetry of the equilibrium action functional, in the same manner as conser-

vation of energy. The only requirements are reversibility, expressed as the equivalence to equilibrium, finite temperature, and spontaneously broken time-translation invariance, which defines the engine cycle. Recovery of Carnot's theorem from the correct, minimal set of physical conditions will be argued to validate the mapping from the reversible engine to its equivalent equilibrium representation, and the symmetries uncovered may provide a starting point for analysis of dissipative cases.

C. Phonon engines at finite temperature

Much of the practical interest in thermoacoustic engines is due to their simplicity [4]; realistic working fluids are near-ideal gases and a wide neighborhood of onset is well described with linear acoustics and second-order, mean-field transport. *All* relevant excitations are thus phonons, with resonator modes and the statistical fluctuations that define the ideal gas differing only in scale. A simple requirement of consistency, that all phonons be defined on the same configuration space, induces the Noether symmetry leading to Carnot's theorem.

The field theory for fixed-temperature ideal gas is defined on a complex, periodic “time cylinder” by the Matsubara construction [21]. Its analytic coordinate is $t - i\tau$, t denoting physical time and τ periodic at the inverse temperature. An analysis of the simplified, reversible thermoacoustic cycle is presented below, in Sec. II, which extends this construction to include all modes in the engine/reservoir system on an equal footing.

Any assumption of reversibility implicitly requires that integration over small-scale statistical fluctuations lead to corrections that can be absorbed into a conservative effective action. The action satisfying this requirement locally for the ideal gas is given in Sec. II A. The reservoir and stack couplings that define a thermoacoustic engine from a simple ideal gas resonator are then introduced in Sec. II B and the whole-engine dynamics derived in two appendixes. That analysis shows both that a nontrivial engine cycle is preserved in a well-defined reversible limit and how phenomenological couplings, first introduced in the equations of motion, can be incorporated as Lagrange multipliers to extend the local action for the ideal gas to a variational description of the whole engine/reservoir system.

A further consistency requirement is then imposed in Sec. III: that the coordinate slicing and associated current conservation laws of the local Matsubara manifold be extendible globally. This requirement identifies the change of field variables representing the reversible engine as an equilibrium critical system, in Sec. III A. The conservation law associated with spontaneous time-translation breaking is then shown to be Carnot's theorem, proved in a general form in Sec. III B. That the one universal theorem for reversible engines is implied by precisely these consistency conditions is taken as their *a posteriori* justification and also as a check on the assumption of reversibility.

The relation of Q scaling to the Ginzburg-Landau description of the equilibrium system and the way the classical equivalence to equilibrium would become inadequate for a reversible engine with a nonzero critical temperature are discussed briefly in Sec. IV.

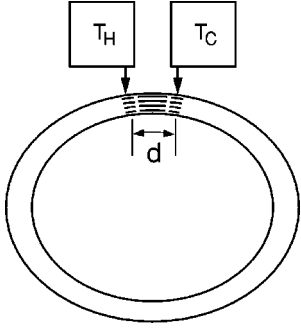


FIG. 1. Geometric arrangement of the annular thermoacoustic stack engine. Short parallel lines beneath the arrows represent heat exchangers and the longer parallel lines represent the prime mover stack. Squares represent reservoirs at the indicated temperatures.

II. VARIATIONAL DESCRIPTION OF THE ACOUSTIC STIRLING ENGINE

Before approaching Carnot's theorem in general terms, it is necessary to show that a reversible, all-phonon engine is definable, has onset properties representing the more general case, and can be described completely with an action principle. This is not possible (in any elementary way) for the intrinsically irreversible, standing-wave "thermoacoustic cycle" [3,4], which is driven by phase-lagged conduction transverse to the gas flow, in a finite-width boundary layer. Ceperley observed [7], however, that the different pressure/velocity phasing of traveling waves transports heat by a Stirling cycle [22], so in principle an annular resonator can be driven reversibly at finite work flux [23]. The driving conduction will be seen to be in phase with temperature fluctuations and thus compatible with variational representation, as expected for a reversible cycle.

The Ceperley engine is shown schematically in Fig. 1. An annular resonator of circumference L , filled with an ideal gas, is connected thermally to two reservoirs at temperatures T_H and T_C and otherwise mechanically and thermally isolated. The connection is through heat exchangers a distance $d \ll L$ apart, at either end of a prime mover stack.

The Ceperley stack resembles the standing-wave stack [4] except that pure in-phase conduction takes place only at the base of thermal boundary layers, so the stack plate spacing must be assumed much smaller than the thermal penetration depth. The idealized stack function in the Stirling limit is to enforce a constraint of fixed temperature. Viscosity and impedance mismatches from complex flow, either in the stack or around the annulus, will be ignored [24]. Because conductive structure transverse to the gas flow is not needed, the resonator may be modeled as a periodic, one-dimensional volume of ideal gas; with appropriate parameter choices below, this description will then be extended to include all parts of the engine.

A. Action for the adiabatic ideal gas

The variational description of the adiabatic ideal gas is simplest in Lagrangian coordinates. Time is labeled t and position in the gas is labeled by an accumulated mass coordinate m , from some arbitrary comoving origin (i.e., for a position x in the annulus, $m \equiv \int^x \rho dx \text{ mod } M$, where ρ is the mass density as a function of position and time and M is the

total mass of gas). In Lagrangian coordinates, $x(t, m)$ is a dynamical embedding field and $\rho \equiv (\partial x / \partial m)^{-1}$. The local velocity $v \equiv (dx/dt)_m$ and the convective derivative is $(d/dt)_m = (\partial/\partial t)_x + v(\partial/\partial x)_t$. It follows that $(\partial/\partial x)_t = \rho(\partial/\partial m)_t$; subscripts may now be omitted without ambiguity and the continuity equation is a tautology:

$$\frac{d\rho}{dt} = \frac{d}{dt} \left(\frac{1}{\partial x / \partial m} \right) = -\rho^2 \frac{d}{dt} \left(\frac{\partial x}{\partial m} \right) = -\rho \left(\frac{\partial v}{\partial x} \right). \quad (1)$$

For particle mass μ and Boltzmann's constant k_B , units with $k_B/\mu = 1$ will be assumed.

Inviscid, nonconductive equations of motion and a constraint of adiabatic evolution are generated by the effective action

$$S = \int dt \oint dm \left\{ \frac{v^2}{2} - \frac{T}{\gamma-1} + T \left[\frac{1}{\gamma-1} \ln \frac{T}{T_0} - \ln \frac{\rho}{\rho_0} \right] \right\}. \quad (2)$$

(The m integral is periodic when describing the resonator gas.) Variation of Eq. (2) with respect to x gives

$$\frac{dv}{dt} = -\frac{\partial}{\partial m}(\rho T), \quad (3)$$

identifying the equation of state $p = \rho T$. Variation with respect to T gives conservation of the specific entropy at comoving coordinate m ,

$$s - s_0 \equiv \frac{1}{\gamma-1} \ln \frac{T}{T_0} - \ln \frac{\rho}{\rho_0} = 0. \quad (4)$$

The action (2) may be *defined* by the requirement that it recover these equations of motion and constraint, but it is also the analytic continuation of the usual free energy, except that x and T may vary, subject to the constraint (4). The continuation is performed by rotating $t \rightarrow -i\tau$ to give the Euclidean action

$$\begin{aligned} -iS \rightarrow S_E &= \int d\tau \oint dm \left\{ \frac{1}{2} \left(\frac{dx}{d\tau} \right)^2 + \frac{T}{\gamma-1} \right. \\ &\quad \left. - T \left[\frac{1}{\gamma-1} \ln \frac{T}{T_0} - \ln \frac{\rho}{\rho_0} \right] \right\} \\ &= \int d\tau \oint dm [u - Ts] + \left(\int d\tau k_B T \right) N s_0. \end{aligned} \quad (5)$$

$N = \oint dm / \mu$ is the number of particles and the internal energy of the gas (kinetic energy plus enthalpy) is $u = (dx/d\tau)^2/2 + T/(\gamma-1)$. If the coordinate τ is made periodic with period $\beta = 1/k_B T$, then $S_E \rightarrow \beta F$, where F is the usual free energy of the microcanonical ensemble, up to additive constants that do not depend on T or x . $1/(\gamma-1) \equiv n/2$, where n is the number of independent degrees of freedom in the usual equipartition computation of the thermodynamic free energy [25]. Thus $\gamma \equiv c_p/c_v$ has the correct dependence on n [20].

The field theory based on Eq. (5) has the Matsubara form [21]. $(dx/d\tau)^2/2$ may be recognized as the specific kinetic energy density of the free phonon gas and is the only term in a “bare” free-phonon action. Correlations in an effective theory for long-wavelength modes are obtained by integration over the short-wavelength statistical fluctuations. At uniform temperature and $x=0$, this average produces the equilibrium free energy F , the form of which shows that both the correction to the specific energy density u and the specific entropy s are local quantities. If the average is performed as an operator expansion about slowly varying x , the same local terms correct the bare equations of motion generated by the free-phonon action [26]. For a nondissipative system, however, it must be possible to reabsorb these corrections into the effective action, and local correspondence with the equation of state generated by the equilibrium free energy then requires that action to take the form (5). (In other words, one can define the nondissipative, variable- x, T action as the sum of actions for ideal gas parcels, separated by imaginary insulating boundaries, so that the compression of each parcel by the walls of its neighbors is that of an equilibrium ideal gas.) The Matsubara condition that all correlations on the Euclidean τ contour continue analytically to t then implies that the Euclidean effective action generating them continues to the dynamical form (2). Requiring that this representation be invariant, up to scale changes, irrespective of where the division between dynamical and statistical phonons is drawn, is equivalent to requiring a scale-invariant treatment of all phonons in the system.

B. Addition of conductivities

As noted, one expects that although the Ceperley cycle requires conductive effects, in the reversible limit only those that can be incorporated in modifications of the actions (2) and (5) should be needed. However, dissipative conductivity is useful as a regulator when solving the equations of motion and extends the solutions to encompass a range of more physically realistic models. Therefore, both conservative and dissipative conductivities will be included temporarily in the dynamical equations and the dissipative terms taken to zero at the end. The main resonator may be given a simple phenomenological bulk conductivity, while conductive effects in the stack are defined from the outset in terms of the desired constraint of nonfluctuating temperature.

The evolution of the internal energy of some comoving region of the gas follows from the equation of motion (3):

$$\begin{aligned} & \frac{d}{dt} \int_{m_1}^{m_2} dm \left(\frac{v^2}{2} + \frac{T}{\gamma-1} \right) \\ &= \int_{m_1}^{m_2} dm \left\{ -v \frac{\partial}{\partial m} (\rho T) + T \frac{d \ln \rho}{dt} + T \frac{ds}{dt} \right\} \\ &= \int_{m_1}^{m_2} dm \left\{ -\frac{\partial}{\partial m} (v \rho T) + T \frac{ds}{dt} \right\} \\ &= \int_{x(m_1, t)}^{x(m_2, t)} dx \left\{ -\frac{\partial}{\partial x} (v \rho T) + \rho T \frac{ds}{dt} \right\}. \end{aligned} \quad (6)$$

Bulk conductivity and source coupling specify the form of

the second term on the right-hand side of Eq. (6). Energy is conserved whenever $\rho T ds/dt = -\partial j_{\text{cond}}/\partial x$, for an arbitrary conduction current j_{cond} . The first term on the right-hand side of Eq. (6) is the divergence of the work flux current $v \rho T$. The convected enthalpy current $\rho v T/(\gamma-1)$ comes from expanding the convective derivative on the left-hand side. Convected kinetic energy is of order v^3 and will be ignored.

Away from the stack, energy is conserved and the standard phenomenological conduction current is

$$j_{\text{cond}} = -\frac{\kappa \gamma}{\gamma-1} \rho \frac{\partial T}{\partial x}, \quad (7)$$

where κ is the thermal diffusivity [4]. (It is convenient to define a rescaled diffusivity $\tilde{\kappa} \equiv \kappa \gamma$, absorbing the ratio of specific heats, to reduce later notation.)

The constraint $\partial T/\partial t = 0$ of perfect thermal coupling, assumed to hold in the interior of the stack, does not conserve comoving enthalpy. Therefore, as observed for both Stirling and more weakly coupled stacks [8,9], longitudinal conduction in the stack cannot be assumed to vanish. It can, however, be idealized as providing exactly the backward heat transport required to compensate for the gain in the stack, which is the implicit content of the constraint. The net effect of conductivity in the stack will therefore be represented with a simple weight function $\sigma(x)$ to give the relative contributions of adiabatic and isothermal evolution of the entropy,

$$\begin{aligned} (\gamma-1) \rho T \frac{ds}{dt} &= \frac{\partial}{\partial x} \left(\tilde{\kappa} \rho \frac{\partial T}{\partial x} \right) (1-\sigma) \\ &+ \left[\rho v \frac{\partial T}{\partial x} + (\gamma-1) \rho T \frac{\partial v}{\partial x} \right] \sigma. \end{aligned} \quad (8)$$

To solve for the behavior of the engine, σ will be taken as a simple scalar function, identically 1 inside the stack, identically 0 outside the heat exchangers, with some smooth transitional behavior between the two regions. If σ is nearly a step function, boundary layer effects will define the physical coupling dynamically, independently of the detailed form assumed. To then relate the solutions to symmetries of the ideal gas, the scalar function will be replaced with a dynamical representation of the local reservoir positions along the stack and an equivalent implementation of $\sigma(x)$ in the action, via Lagrange multipliers.

C. Stability and transport results

The wave equation is the time derivative of Eq. (3):

$$\frac{d^2 v}{dt^2} = \frac{\partial}{\partial m} \left(\gamma \rho T \frac{\partial v}{\partial x} - (\gamma-1) \rho T \frac{ds}{dt} \right) \quad (9)$$

(recovering the speed of sound for small perturbations as $\gamma k_B T = \mu c^2$ when $ds/dt=0$). Its solution with the entropy evolution of Eq. (8) gives the stability properties of resonator modes. For the annular engine, however, the absence of pressure boundaries makes imposed temperature gradients a

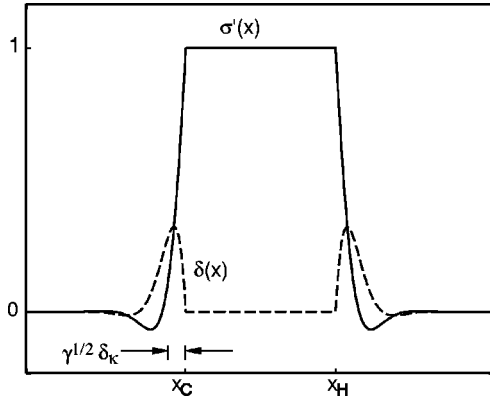


FIG. 2. Form of the boundary-layer coupling functions σ' and δ .

more important impedance discontinuity than they are for standing waves [9], so the phasing of the modal eigenvectors cannot be assumed *a priori*.

Equations (8) and (9) will therefore be solved self-consistently to second order in small sound pressures. With angular brackets denoting the time average of any quantity over some complete number of cycles, the mean and oscillatory parts of the temperature field are given in terms of v by the average of Eq. (8) outside the stack:

$$\left\langle \frac{\partial}{\partial x} \left(\tilde{\kappa} \rho \frac{\partial T}{\partial x} \right) \right\rangle = \left\langle \rho \left(\frac{\partial T}{\partial t} + v \frac{\partial T}{\partial x} \right) + (\gamma - 1) T \frac{\partial v}{\partial x} \right\rangle. \quad (10)$$

Vanishing of linear-order oscillations relates temperature to velocity fluctuations and the static mean temperature is then solved in terms of the transport invariants around the annulus, represented by the cycle averages of second-order quantities as in Ref. [4]. The algebra for these steps is performed in Appendix A.

The resulting static background T is then substituted into Eq. (9), which is solved as an eigenvalue-eigenvector problem at linear order to find the independent modes v and their frequencies in Appendix B. The mean temperature solutions of Eq. (10) are parametrized by sound intensity, convected mass transport, and a parameter α , which measures the ratio of standing to traveling components in the eigenfunction and the standing component phase. In general, they do not correspond to purely real frequencies for the oscillating components, so small instabilities are assumed, to permit sensible cycle averages.

At nonzero dissipative conductivity, boundary layers at the ends of the stack are found to extend the original, real-valued coupling strength σ to a complex coupling ($\sigma' - i\delta$), given in Eq. (A7) and shown in Fig. 2. The real part of the difference $\sigma' - \sigma$ merely hides the detailed form of the coupling function at the stack ends in a conductive transition region. This thermal averaging will be exploited below to model the stack region as a set of discrete, mutually decoupled thermal reservoirs (Swift's "bucket brigade" [4], though for the Stirling cycle), each tied by a δ function of temperature to the instantaneously adjacent volume of gas in the resonator.

The imaginary part of the dynamical coupling $i\delta$ performs an interesting refrigeration cycle in realistic models,

which is relevant to the saturation value of the sound intensity Λ . However, because δ , a dissipative, pure loss term, is not needed to define the working cycle, it can be eliminated by taking $\tilde{\kappa} \rightarrow 0$. As long as the stack plate spacing remains smaller than the boundary layer thickness $\sqrt{\gamma \delta \kappa} \equiv \sqrt{2 \tilde{\kappa} / \omega}$ in the limit, $\sigma' \rightarrow \sigma$, but otherwise the conductive coupling remains unchanged.

The final result of the appendixes is that the scaling dependence of the quality factor on the temperature difference $T_H - T_C$ and on mode number is the same as for the standing-wave case [6]. The quality factor Q is defined from the imaginary part of the modal eigenfrequency for each mode, as given in Eq. (B17), by

$$-\frac{1}{Q} \equiv \frac{d \ln \Lambda}{\omega dt} = \frac{-2 \operatorname{Im}(\omega)}{\omega}. \quad (11)$$

For perturbations about $\Lambda = 0$, Eqs. (B17) and (11) reduce at leading order in $(T_H - T_C)/T_C \equiv \Delta T/T$ to $-1/Q = \Delta T/2\pi j \gamma T$ for mode j , giving a growth time independent of mode number. Corrections from effects such as bulk conductivity and losses in boundary layers δ of finite thickness, as given in Eq. (B16), modify the reversible result to

$$-\frac{1}{Q} = \frac{1}{2\pi j} \frac{\Delta T - T_{\text{crit}}}{\gamma T}, \quad (12)$$

where $T_{\text{crit}}/T = \alpha(\gamma - 1)k_j \sqrt{\gamma \delta \kappa}(\omega)$ and k_j is the wave number of the j^{th} mode in the resonator. Therefore, modes with either steeper velocity gradients or greater projection of those gradients onto the boundary regions also suffer larger critical temperatures to onset. This too is in qualitative agreement with the results of Ref. [5]. Though this model omits too many physical effects for more direct comparison to be meaningful, it does show that the qualitative dependence of modal onset parameters on various gain and loss effects is similar for the traveling-wave and the standing-wave cycles, when both operate in irreversible regimes.

III. REVERSIBILITY AS EQUILIBRIUM

In Eq. (5), the periodicity of the Matsubara manifold was defined in terms of the temperature T . This prescription is straightforward for isothermal equilibrium systems, but not obviously sensible if T is a dynamical field, because then the coordinates for fluctuations are defined in terms of the fluctuations themselves. Yet the adiabatic changes of state in a reversible transformation strongly resemble otherwise meaningless scale transformations in the description of an equilibrium system. Therefore, it should be possible to ensure well-defined coordinate slicing of the Matsubara manifold, while admitting temperature fluctuations, by regarding temperature as a metriclike scale factor and different states of the adiabatic ideal gas as identical up to classical rescalings of some canonical base manifold. The transformation from physical embedding coordinates to the canonical base manifold defines the equivalent equilibrium system and assumes physical significance of the new conservation law associated with scale transformations.

A. The equivalent equilibrium system

One may transform Lagrangian coordinates from (t, m) to a new set (z, m) , with $\partial t / \partial z|_m \equiv \beta / \beta_0$, to place Eq. (2) in an equivalent form

$$S[t, x] = \int dz \int dm \left\{ \frac{1}{2} \frac{(\partial x / \partial z|_m)^2}{(\partial t / \partial z|_m)} + T_0 \left[\ln \left(\rho_0 \frac{\partial(t, x)}{\partial(z, m)} \right) - \frac{\gamma}{\gamma-1} \ln \left(\frac{\partial t}{\partial z} \Big|_m \right) - \frac{1}{\gamma-1} \right] \right\}. \quad (13)$$

Here $\partial(t, x) / \partial(z, m) \equiv [\partial t / \partial z|_m \partial x / \partial m|_z - \partial x / \partial z|_m \partial t / \partial m|_z]$ is the Jacobian of the transformation, (z, m) define the canonical base manifold, and (t, x) embed it into real space and time. x and $\partial z / \partial t|_m = T / T_0$ may be regarded as the fundamental dynamical fields or at the price of introducing an additional, lower-dimensional degree of freedom in the initial conditions for t , the full embedding coordinates (t, x) may be used.

It is now natural to treat the dilation from t to z as a Weyl transformation on the complex time manifold and rather than rotating $t \rightarrow -i\tau$ to continue $z \rightarrow -i\zeta$. If $\partial t / \partial z|_m \equiv \partial \tau / \partial \zeta|_m$ defines an analytic function of $z - i\zeta$, then $\oint d\zeta = \beta_0$ everywhere corresponds to the previous relation $\oint d\tau = \beta$ for a locally ideal gas with slowly varying temperature. The Euclidean continuation of Eq. (5) then becomes

$$S_E[\tau, x] = \oint d\zeta \int dm \left\{ \frac{1}{2} \frac{(\partial x / \partial \zeta|_m)^2}{(\partial \tau / \partial \zeta|_m)} - T_0 \left[\ln \left(\rho_0 \frac{\partial(\tau, x)}{\partial(\zeta, m)} \right) - \frac{\gamma}{\gamma-1} \ln \left(\frac{\partial \tau}{\partial \zeta} \Big|_m \right) - \frac{1}{\gamma-1} \right] \right\}. \quad (14)$$

Equation (14) separates field fluctuations associated with particular solutions from the coordinate slicing of the surface on which they are defined. As a result, lack of an explicit ζ or m dependence in the action implies conservation of currents across constant- ζ or $-m$ surfaces, which are now well defined, via Noether's theorem.

The lapse component $\partial \tau / \partial \zeta|_m$ of the embedding, relating temperature T to a canonical reference temperature $T_0 = 1/k_B \beta_0$, may also now be dynamically constrained. If a Lagrange multiplier is added to set $\partial \tau / \partial \zeta|_m$ constant, Eq. (14) reverts to Eq. (5), describing isothermal sound. A closed volume, so constrained, becomes an ideal-gas reservoir. The stack can be similarly represented and the scalar coupling σ replaced with a series of local constraints, giving a fully variational description of the engine/stack/reservoir system.

The Ceperley engine is thus modeled, as shown in Fig. 3, as a collection of one-dimensional regions of ideal gas. $N + 1$ separate volumes are labeled with mass coordinates $\{m_0, \dots, m_N\}$. The finite, periodic region m_0 is the resonator, two semi-infinite regions $m_1 \in (-\infty, 0)$ and $m_N \in (0, \infty)$ will be respectively hot and cold reservoirs, and finite volumes $\{m_2, \dots, m_{N-1}\}$ represent thermal repository positions along the stack. If larger values of $n_j / 2 \equiv 1 / (\gamma_j - 1)$ are chosen in regions $j = 1, \dots, N$ than for $j = 0$, the specific heat in the reservoirs and stack can be made arbitrarily large and thermal fluctuations suppressed to any desired degree,

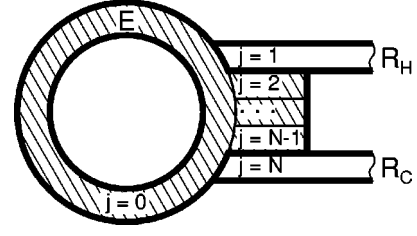


FIG. 3. Schematic representation of the annular engine as a collection of one-dimensional ideal gas regions. The reservoirs (R_H, R_C) and engine (E) are demarcated by the heavy solid lines. The engine (shaded) comprises the resonator ($j=0$) and volumes $j=2$ to $N-1$ representing the stack. The reservoir coupling to external, isothermal sources at infinity is indicated by the wavy lines.

relative to those of adiabatic sound in the resonator. In this way, isothermal constraints are arbitrarily well approximated.

A constraint action is then introduced to equate the temperature of the gas instantaneously at a point in the resonator to that of a component of the stack or a reservoir:

$$S_C \equiv \oint d\zeta \sum_{j=1}^N \lambda_j \left[\int dm_0 \frac{\partial \tau_0}{\partial \zeta} \delta(x_0 - x_j^0) - \int dm_j \frac{\partial \tau_j}{\partial \zeta} \delta(x_j - x_j^0) \right] + i \oint d\zeta \lambda_H \int dm_1 \delta(x_1 + \infty) \left(\frac{\partial \tau_1}{\partial \zeta} - \beta_H \right) + i \oint d\zeta \lambda_C \int dm_N \delta(x_N - \infty) \left(\frac{\partial \tau_N}{\partial \zeta} - \beta_C \right). \quad (15)$$

Here $\delta(x_0 - x_j^0)$ is some highly peaked, nonlinear function of the embedding coordinate $x_0(\zeta, m_0)$, resembling a Dirac delta function, and the x_j^0 are a sequence of constants representing positions at the heat exchangers and along the stack. Since x_0 and τ_0 are both functions of any given point (ζ, m_0) , the auxiliary field λ_j enforces a constraint on $\partial \tau_0 / \partial \zeta$ only when the spatial coordinate x_0 also takes value x_j^0 . Similarly, the δ functions in the stack and reservoir regions constrain their temperatures at individual positions x_j^0 , which in the following analysis are arbitrary. Finally, two δ functions, at $x_1 = -\infty$ and $x_N = \infty$, place the asymptotes of the reservoirs at constant lapse (inverse temperature) $\beta_H \equiv 1/T_H$ and $\beta_C \equiv 1/T_C$, respectively.

Derivations of Carnot's theorem traditionally employ an external mechanical load, coupled by a work term $p dV$ to the working fluid of the engine (where p is pressure and V is some variable volume), to accumulate work while allowing a perfectly repeatable engine cycle. The formal device of such a load will not be used here because the driven sound mode in the resonator serves the dual purpose of both load and transport apparatus. Its internal energy, proportional to Λ in the range of linear perturbations, measures work done on, rather than by, the engine. The lack of a precisely periodic cycle in time will present no difficulties because energy will be identified in the following derivation as the conserved current associated with time-translation symmetry and its re-

lation to heat flow shown identically, irrespective of how it is partitioned among system excitations.

B. Carnot's theorem

The constrained Euclidean action $S_E[\{\tau, x\}_j] + S_C[\{\tau, x, \lambda\}_j]$ is taken here to be the fundamental object encoding the degrees of freedom, symmetries, and conservation laws of the reversible annular engine. Symmetry breaking follows as a corollary because $S_E + S_C$ is equally the source of engine dynamics, or β_0 times the free energy of a nondynamical system in thermal equilibrium. The kinetic term in (ζ, m) variables is nonquadratic, so its direct solution together with the constraints is cumbersome. For that reason only, one uses the *device* of rotation $\zeta \rightarrow i z$ and the transformation of coordinates from (z, m) to (t, m) to find the extremal solutions. Under analytic continuation back to ζ , though, these must still be the classical minima of the equilibrium free energy. Such an interpretation might seem contrived, except that the Euclidean conservation laws in coordinates (ζ, m) are precisely those for the entropy flux expressed in Carnot's theorem, as will now be shown.

The only assumptions will be that an action exists with a Weyl symmetry like that of temperature fluctuation above and that the minima of the free energy are nonunique and form a continuous, degenerate set. The last condition is nothing more than the statement that the action $S_E + S_C$ has a spontaneously broken symmetry, in keeping with the equilibrium critical interpretation.

To condense notation, let ξ represent the set of dynamical fields of the theory (the $\{x_j\}$, $\{T_j\}$ and $\{\lambda_j\}$). A single coordinate m will be used to represent the entire set of positions $\{m_j\}$. Because the cases discussed here only involve two reservoirs, it is convenient to use $-\infty \leq m \leq m_-$ to denote positions in the hot reservoir further away than some point adjacent to the engine and similarly $m_+ \leq m \leq \infty$ for the asymptotic region of the cold reservoir. The remaining $m_- \leq m \leq m_+$ are used to denote the parts of these reservoirs adjacent to the engine and all positions in the resonator and stack. Departing from the convention above, to adopt a notation more natural to Noether's theorem, coordinate differentiation will be indicated with plain derivatives and partials will be reserved for differentiation of Lagrangians with respect to field arguments. Subscripts will indicate which coordinates are being used.

Proof. First, one writes the same action in both coordinates (t, m) and (z, m) , with $dt/dz|_m \equiv \beta/\beta_0$, as above:

$$\begin{aligned} S &= \int dt \int dm \mathcal{L} \left(\xi, \frac{d\xi}{dt} \Big|_m, \frac{d\xi}{dm} \Big|_t, \dots \right) \\ &= \int dz \int dm \lambda \left(\xi, \frac{d\xi}{dz} \Big|_m, \frac{d\xi}{dm} \Big|_z, \dots \right). \end{aligned} \quad (16)$$

(The ellipses stand for terms involving higher orders in derivatives that could be admitted more generally.) It follows that, as densities, $\lambda = (\beta/\beta_0)\mathcal{L}$. The continuation $z \rightarrow -i\zeta$ and periodic identification gives

$$S_E = \oint d\zeta \int dm \lambda_E \left(\xi, \frac{d\xi}{d\zeta} \Big|_m, \frac{d\xi}{dm} \Big|_\zeta, \dots \right). \quad (17)$$

If, as above, the eigenvalue analysis of the dynamical variation of S shows that time translation symmetry is broken by the ground state of S_E , it follows that given a ground state solution ξ , the transformation $\xi \rightarrow \xi + (\epsilon/\beta)d\xi/d\zeta|_m$, with ϵ constant, produces another of the degenerate ground states, with no change of action,

$$\begin{aligned} \delta_{\text{sym}} S_E = 0 &= \oint d\zeta \int_{-\infty}^{\infty} dm \epsilon \left\{ \frac{1}{\beta} \frac{d\xi}{d\zeta} \Big|_m \frac{\partial \lambda_E}{\partial \xi} + \frac{d}{d\zeta} \Big|_m \left(\frac{1}{\beta} \frac{d\xi}{d\zeta} \Big|_m \right) \right. \\ &\quad \times \frac{\partial \lambda_E}{\partial (d\xi/d\zeta|_m)} + \frac{d}{dm} \Big|_\zeta \left(\frac{1}{\beta} \frac{d\xi}{d\zeta} \Big|_m \right) \frac{\partial \lambda_E}{\partial (d\xi/dm|_\zeta)} \\ &\quad \left. + \dots \right\}. \end{aligned} \quad (18)$$

Of course, δS_E vanishes for general variation about a stationary point, by the Euclidean equations of motion. Choosing as one such "dynamical" variation $\xi \rightarrow \xi + (\epsilon/\beta)d\xi/d\zeta|_m$, with ϵ constant for $m_- \leq m \leq m_+$ and zero otherwise, gives the null variation

$$\begin{aligned} \delta_{\text{dyn}} S_E = 0 &= \oint d\zeta \int_{m_-}^{m_+} dm \epsilon \left\{ \frac{1}{\beta} \frac{d\xi}{d\zeta} \Big|_m \frac{\partial \lambda_E}{\partial \xi} + \frac{d}{d\zeta} \Big|_m \left(\frac{1}{\beta} \frac{d\xi}{d\zeta} \Big|_m \right) \right. \\ &\quad \times \frac{\partial \lambda_E}{\partial (d\xi/d\zeta|_m)} + \frac{d}{dm} \Big|_\zeta \left(\frac{1}{\beta} \frac{d\xi}{d\zeta} \Big|_m \right) \frac{\partial \lambda_E}{\partial (d\xi/dm|_\zeta)} \\ &\quad \left. + \dots \right\} - \oint d\zeta \epsilon \left(\frac{1}{\beta} \frac{d\xi}{d\zeta} \Big|_m \right) \frac{\partial \lambda_E}{\partial (d\xi/dm|_\zeta)} \Big|_{m_-}^{m_+}. \end{aligned} \quad (19)$$

The difference of Eq. (19) from Eq. (18) contains only surface integrals:

$$\begin{aligned} 0 &= \oint d\zeta \left(\int_{-\infty}^{m_-} dm + \int_{m_+}^{\infty} dm \right) \epsilon \left(\frac{d\lambda_E}{d\zeta} \Big|_m \right) \\ &\quad + \oint d\zeta \frac{\epsilon}{\beta} \left(\frac{d\xi}{d\zeta} \Big|_m \frac{\partial \lambda_E}{\partial (d\xi/dm|_\zeta)} \right) \Big|_{m_-}^{m_+}. \end{aligned} \quad (20)$$

The practical definition of a reservoir has been assumed (an asymptotic region in which the temperature can be taken as constant), making it possible to pull the factors of β out of ζ derivatives. In regions of constant β , the translation in ζ is, under the analytic continuation to z , simply proportional to the translation in t . Time-translation symmetry of the theory follows from the absence of explicit t dependence in the action, which in the reservoirs implies the absence of an explicit ζ dependence. (The Ceperley example above demonstrates these features.) The first ζ integral of Eq. (20) thus contains a total derivative on a periodic domain and vanishes identically.

The remaining average end point currents in ζ coordinates [with the definition $\langle J \rangle \equiv \oint d\zeta J(\zeta)/\oint d\zeta$ of averages] must cancel,

$$\frac{1}{\beta} \left\langle \frac{d\xi}{d\zeta} \left| \frac{\partial \lambda_E}{\partial (d\xi/dm|_{\zeta})} \right| \right\rangle_{m_-}^{m_+} = 0. \quad (21)$$

This average, however, is just the zero-frequency coefficient in the Fourier expansion of these currents on the domain of ζ . An analytic continuation from ζ to z is simply an expansion in complex exponentials with contour-independent coefficients (including the zero mode), implying that

$$\frac{1}{\beta} \left\langle \frac{d\xi}{dz} \left| \frac{\partial \lambda}{\partial (d\xi/dm|_z)} \right| \right\rangle_{m_-}^{m_+} = 0. \quad (22)$$

A parallel application of Noether's theorem to the global time-translation symmetry can be carried out in the coordinates (t, m) . The t independence of \mathcal{L} gives zero variation under a constant shift and for a more general time- and space-dependent shift $\tilde{\epsilon}$, the counterpart to Eq. (19) is

$$\begin{aligned} \delta_{\text{dyn}} S = 0 &= \int dt \int_{m_-}^{m_+} dm \tilde{\epsilon} \left\{ \xi \left[\frac{\partial \mathcal{L}}{\partial \xi} - \frac{d}{dt} \left| \frac{\partial \mathcal{L}}{\partial \dot{\xi}} \right| \right] \right. \\ &\quad \left. + \frac{d\xi}{dm} \left| \frac{\partial \mathcal{L}}{\partial \xi'} \right| + \dots \right\} - \int dt \tilde{\epsilon} \left(\xi \frac{\partial \mathcal{L}}{\partial \xi'} \right)_{m_-}^{m_+} \\ &= \int dt \tilde{\epsilon} \int_{m_-}^{m_+} dm \left(- \frac{d\mathcal{H}}{dt} \right)_{m} - \int dt \tilde{\epsilon} \left(\xi \frac{\partial \mathcal{L}}{\partial \xi'} \right)_{m_-}^{m_+}. \end{aligned} \quad (23)$$

Here $\tilde{\epsilon}$ has been chosen constant in m between m_- and m_+ , but a general function of t vanishing at $t \rightarrow \pm\infty$, and the shorthand $\dot{\xi} \equiv d\xi/dt|_m$, $\xi' \equiv d\xi/dm|_t$ is introduced. The Hamiltonian \mathcal{H} is defined by the terms appearing in curly brackets in Eq. (23). The simple form of the kinetic term in the (t, m) coordinates gives, for the action of the previous sections, $\mathcal{H} = \xi \partial \mathcal{L} / \partial \dot{\xi} - \mathcal{L}$. Because \mathcal{L} contains logarithmic terms representing the entropy, however, in the general case \mathcal{H} represents the full "free-energy density" of the gas in the engine. [If the device of a separately variable mechanical regulator load had been assumed, to allow the engine behavior to be truly cyclic, the total derivative of that part of \mathcal{H} representing the engine could have been chosen to vanish over complete cycles and $\int dt \int_{m_-}^{m_+} dm (d\mathcal{H}/dt|_m)$ would simply be the work done on the load.] The end point terms are thus identified as the energy flux currents at the reservoir boundaries (heat flux currents for $m_{\pm} \rightarrow \pm\infty$ and coupling only to thermal sources). Therefore, writing $J_E(t, m) \equiv \xi \partial \mathcal{L} / \partial \dot{\xi}'$ and recalling that $d\xi/dz|_m = (\beta/\beta_0)\dot{\xi}$, $\lambda = (\beta/\beta_0)\mathcal{L}$, and in regions of constant β , $d/dm|_z = d/dm|_t$, it follows that

$$\frac{\beta_0}{\beta} \left(\frac{d\xi}{dz} \left| \frac{\partial \lambda}{\partial (d\xi/dm|_z)} \right| \right) = \frac{\beta}{\beta_0} J_E. \quad (24)$$

From the constant-temperature heat flux relation $dQ = T dS$, βJ_E can be recognized as the entropy flux current. A convenient variation (23) is defined by $\tilde{\epsilon} = \text{const}$ on (t_-, t_+) , where $(t_+ - t_-)$ is an integral number of engine cycles, and $\tilde{\epsilon} = 0$ otherwise. It then follows from Eq. (22), Eq. (23), and the definition of the time average as the zero-frequency Fourier component that

$$\begin{aligned} &\int_{t_-}^{t_+} dt \int_{m_-}^{m_+} dm \left(\frac{d\mathcal{H}}{dt} \right)_{m} \\ &= \left(\int_{t_-}^{t_+} dt \right) \langle J_E(t, m_-) - J_E(t, m_+) \rangle \\ &= \left(\frac{T_H}{T_C} - 1 \right) \int_{t_-}^{t_+} dt J_E(t, m_+), \end{aligned} \quad (25)$$

which is Carnot's relation between the change in the free energy of the engine (or optionally the load) and the heat flux current into the cold reservoir [20]. Q.E.D.

IV. DISCUSSION: DISSIPATION AND THE CRITICAL INTERPRETATION

The gas equations taken as the starting point in the appendixes result from integration over microscopic fluctuations, while the resonator modes are left explicitly dynamical. Further integration over resonator oscillations, leaving only the evolution of the intensity explicitly dynamical, corresponds to formation of the usual Ginzburg-Landau effective action for the order parameter [18].

The mode power equation (12) for the unstable mode at $\Delta T > T_{\text{crit}}$ can be obtained by variation of the fields in the action

$$S_{\text{GL}} = \int dt \frac{1}{2} \left\{ \frac{dA^*}{dt} \frac{dA}{dt} + \frac{1}{4} \left(\frac{\bar{c}}{L} \frac{\Delta T - T_{\text{crit}}}{\gamma T} \right)^2 A^* A \right\}. \quad (26)$$

Here a complex mode amplitude is defined as $A \equiv \sqrt{\Lambda} e^{i\varphi}$ and φ is the phase of a traveling wave around the resonator, referred to an arbitrary instant of time. (This indexing of the set of degenerate traveling waves correctly provides the uniqueness of modes of different φ at nonzero Λ , together with the smoothness property that perturbations at all φ become identical as $\Lambda \rightarrow 0$.)

Equation (26) may be compared to the action for the canonical "Mexican-hat" symmetry-breaking potential on the complex plane [15],

$$S_{\text{SB}} = \int dt \frac{1}{2} \left\{ \frac{da^*}{dt} \frac{da}{dt} - \mu^2 a^* a - \frac{\lambda}{12} (a^* a)^2 \right\}. \quad (27)$$

Linear perturbation analysis of the heat engine provides only the quadratic terms in Eq. (26); the stabilizing higher-order terms must come from nonlinear evaluation of the self-consistent equations at finite sound amplitude. The effective

coupling determining the strength of the instability around $a=0$ can be read from the correspondence as $-\mu^2 = [(\bar{c}/2L)(\Delta T - T_{\text{crit}})/\gamma T]^2$.

In the classical problem, as μ^2 transits positively through zero, the motion of the field a goes from exponential instability to *oscillatory* stability around $a=0$ and symmetry of the ground state is restored. The irreversible engine with finite T_{crit} has no such regime; it transits from exponential instability above onset to *exponential* stability below. Yet the terms in Eq. (27) through quadratic order, with real μ^2 , are the most general possible for an analytic action with these symmetries, covering both sides of the symmetry-breaking transition.

The only way the reversible Ceperley engine can be equivalent at the *classical* level to an equilibrium system and have action (27) to obtain the dynamics of the broken phase is for $T_{\text{crit}} \rightarrow 0$, as it was found to do in Appendix B. This characteristic thus appears to be a necessary condition on any engine that can undergo onset in the reversible limit. An interesting open question is whether embedding the simple actions considered here in an equilibrium partition function and keeping dissipative (nonanalytic) corrections to the correlation functions correctly recovers nonzero T_{crit} and the exponential decay in the stable regime seen for irreversible engines.

ACKNOWLEDGMENTS

I would like to thank N. Chotiros for providing an opportunity to present a preliminary version of this work at a meeting of the Acoustical Society of America, and A. Atchley for discussions. Financial support was provided by the Depart-

ment of Energy, Office of Basic Energy Science, Engineering and Geoscience Contract No. W7405-ENG-36.

APPENDIX A: TRANSPORT MEAN FIELD AND FLUCTUATIONS

The standing-wave thermoacoustic cycle has been extensively analyzed and modeled [1–4,6,27], with emphasis on quantitative prediction as well as general scaling properties [28]. The traveling-wave engine has received much less attention [7,8] and reflecting limitations in current stack technologies, many treatments have assumed wide-plate, standing-wave-type stacks [9,10], which operate far from the reversible limit and couple weakly to the Stirling cycle [10]. No eigenvalue analysis of annulus modes in the Stirling limit, equivalent to Ref. [2] for standing waves, has been performed; nor has back reaction from thermal transport been considered to complete the treatment of the idealized stack [8].

A self-contained stability and transport analysis is therefore presented in this and the following appendix. Because its ultimate purpose is to demonstrate the relation between a reversible thermoacoustic limit and global variational principles, the effects of dissipative versus conservative conductivity will be carefully distinguished. The back reaction is considered in some detail because, together with *stack-end* boundary layers, it creates mode-dependent critical temperatures qualitatively similar to those for standing-wave engines. Keeping these effects places the reversible limit in context in the more general case.

The mean temperature background is found to second order in small sound amplitude by decomposing the expression (8), assuming forms $T = T_0 + T_1$ and $\rho = \rho_0 + \rho_1$ as functions of x , with the 0-subscripted quantities defined to be static. The background value v_0 will be taken as 0. This gives

$$\left\{ \rho_0 \left[\frac{\partial T_1}{\partial t} + v \frac{\partial T_0}{\partial x} + (\gamma - 1) T_0 \frac{\partial v}{\partial x} \right] = \left\{ 0 + \rho_1 \left[\frac{\partial T_1}{\partial t} + v \frac{\partial T_0}{\partial x} + (\gamma - 1) T_0 \frac{\partial v}{\partial x} \right] + \frac{\partial}{\partial x} \left((\tilde{\kappa} \rho)_0 \frac{\partial T_0}{\partial x} \right) \right. \right. \\ \left. \left. + \rho_0 \left[v \frac{\partial T_1}{\partial x} + (\gamma - 1) T_1 \frac{\partial v}{\partial x} \right] + \frac{\partial}{\partial x} \left((\tilde{\kappa} \rho)_0 \frac{\partial T_1}{\partial x} + (\tilde{\kappa} \rho)_1 \frac{\partial T_0}{\partial x} \right) + \dots \right\} + \dots \right\}. \quad (\text{A1})$$

The oscillatory part at linear order must vanish by itself, giving

$$\rho_0 \left[\frac{\partial T_1}{\partial t} + v \frac{\partial T_0}{\partial x} + (\gamma - 1) T_0 \frac{\partial v}{\partial x} \right] = \frac{\partial}{\partial x} \left((\tilde{\kappa} \rho)_0 \frac{\partial T_1}{\partial x} + (\tilde{\kappa} \rho)_1 \frac{\partial T_0}{\partial x} \right). \quad (\text{A2})$$

For small conductivities and small absolute temperature variations, the temperature and density dependence of $\tilde{\kappa}$ will be ignored, the term $(\tilde{\kappa} \rho)_1$ will be dropped, and $(\tilde{\kappa} \rho)_0$ or $\tilde{\kappa}$ will be treated as constant. $\sqrt{2\tilde{\kappa}/\omega} \equiv \sqrt{\gamma} \delta_\kappa$ defines a diffusion wavelength [29], the thermal boundary layer thickness

for oscillations at frequency ω , and δ_κ is as in Ref. [4]. In terms of δ_κ , the small-conductivity limit for modes with wave number $k \sim 2\pi/L$ is given by

$$\frac{\delta_\kappa}{L} = \sqrt{\frac{\tilde{\kappa}}{\gamma^2 \pi L c}} \ll 1. \quad (\text{A3})$$

Without stack boundaries, Eq. (A2) would be solved by an adiabatic temperature field \tilde{T}_1 , with

$$\frac{\partial \tilde{T}_1}{\partial t} + v \frac{\partial T_0}{\partial x} + (\gamma - 1) T_0 \frac{\partial v}{\partial x} = 0, \quad (\text{A4})$$

up to terms of $O(\delta_\kappa/L)^2$ associated with conductivity in the bulk. To focus attention on the transport properties associated with the stack, quadratic terms in δ_κ/L will be assumed smaller than all terms that are kept.

The adiabatic solution, which does not generally satisfy the boundary condition $T_1=0$ at the stack ends, can be augmented by considering a solution T'_1 of

$$\frac{\partial T'_1}{\partial t} = \tilde{\kappa} \frac{\partial^2 T'_1}{\partial x^2} \quad (\text{A5})$$

of the approximate form

$$T'_1 = -\tilde{T}_1 \left[\Theta_{x < x_C} e^{-(1+i)|x-x_C|/\sqrt{\gamma}\delta_\kappa} + \Theta_{x > x_H} e^{-(1+i)|x-x_H|/\sqrt{\gamma}\delta_\kappa} + O\left(\frac{\delta_\kappa}{L}\right) \right]. \quad (\text{A6})$$

Here Θ are Heaviside functions and the subscripts indicate where Θ takes value 1. The combined function $T_1 = \tilde{T}_1 + T'_1$ satisfies Eq. (A2) up to $O(\delta_\kappa/L)$ and $T_1=0$ at the edges of the stack. It is now natural to define the physical coupling functions

$$\begin{aligned} \sigma' &\equiv \sigma + (1-\sigma) \text{Re} \left[\Theta_{x < x_C} e^{-(1+i)|x-x_C|/\sqrt{\gamma}\delta_\kappa} \right. \\ &\quad \left. + \Theta_{x > x_H} e^{-(1+i)|x-x_H|/\sqrt{\gamma}\delta_\kappa} \right], \\ \delta &\equiv -(1-\sigma) \text{Im} \left[\Theta_{x < x_C} e^{-(1+i)|x-x_C|/\sqrt{\gamma}\delta_\kappa} \right. \\ &\quad \left. + \Theta_{x > x_H} e^{-(1+i)|x-x_H|/\sqrt{\gamma}\delta_\kappa} \right]. \end{aligned} \quad (\text{A7})$$

These functions have the forms shown in Fig. 2. σ' simply extends the conductive region of the stack in a frequency-dependent way and as long as σ is sharper than $\sqrt{\gamma}\delta_\kappa$, its particular form does not matter. δ defines the transition region between adiabatic and isothermal behavior, as will be seen explicitly below. Using these definitions, the correction T_1 to the background can be given everywhere in terms of the adiabatic solution \tilde{T}_1 , as $T_1 = \tilde{T}_1 [1 - (\sigma' - i\delta)]$.

The remaining, second-order contribution to Eq. (A1) must then vanish separately. Only its constant part is considered in the mean-field approximation; for oscillations of v at frequency ω the remaining terms have frequency 2ω . Computing the cycle average of two oscillatory functions a and b from their complex forms as explained in Ref. [4], $\langle ab \rangle = \text{Re}(a^*b)/2$, and solving the continuity equation (1) to leading order to obtain, $\rho_1/\rho_0 = (i/\omega)\partial v/\partial x$, the second-order term can be reduced to

$$\begin{aligned} \frac{\partial}{\partial x} \left((\tilde{\kappa}\rho)_0 \frac{\partial T_0}{\partial x} \right) &= \gamma \langle \rho_1 v \rangle \frac{\partial T_0}{\partial x} - \frac{\rho_0 \langle v^2 \rangle}{\omega} \frac{\partial}{\partial x} \left(\frac{\partial T_0}{\partial x} \delta \right) + (\gamma-1) \\ &\quad \times \left\{ \frac{\rho_0}{\omega} \delta \left[2 \left\langle \left(\frac{\partial v}{\partial x} \right)^2 \right\rangle - \frac{1}{T_0} \frac{\partial T_0}{\partial x} \frac{\partial}{\partial x} \left\langle \frac{v^2}{2} \right\rangle \right] \right. \\ &\quad \left. - \frac{\rho_0}{\omega} \frac{\partial}{\partial x} \left(T_0 \delta \frac{\partial}{\partial x} \left\langle \frac{v^2}{2} \right\rangle \right) \right. \\ &\quad \left. - \langle \rho_1 v \rangle \left[\frac{\partial}{\partial x} (T_0 \sigma') - \frac{\partial T_0}{\partial x} (1 - \sigma') \right] \right\}. \end{aligned} \quad (\text{A8})$$

An approximation consistent with thin boundary layers and no flow impedance in a stack of length $d \ll L$ is that $\langle v^2 \rangle \approx \text{const}$ across the boundary layers and even across the stack. Therefore, a characteristic scale factor for the intensity of sound in the engine is

$$\Lambda \equiv \frac{\langle v^2 \rangle}{\tilde{\kappa}\omega}. \quad (\text{A9})$$

Alternatively written, $\Lambda/2 = \langle (\delta x)^2 \rangle / \gamma \delta_\kappa^2$, where $\langle (\delta x)^2 \rangle$ is the mean squared displacement of fluid due to the sound wave. (For reference, for 500-Hz oscillations of helium, with a sound speed $c \sim 1000$ m/s and $\delta_\kappa \leq 1$ mm, sound pressures $\rho_1/\rho_0 \sim 1\%$ correspond to values of $\Lambda \sim 10$. Therefore, it is conventional to consider gas displacements comparable to the boundary layer thickness sweeping into and out of the ends of the regenerator.)

Integration of Eq. (1) gives the condition for continuity of convective mass transport $\partial/\partial x \langle \rho_1 v \rangle = 0$. Taking $(\tilde{\kappa}\rho)_0$ as a constant, a characteristic wave number for a given traveling-wave solution indexed by an integer j can then be defined as

$$k_j \equiv \frac{\langle \rho_1 v \rangle \tilde{\kappa}\omega}{(\tilde{\kappa}\rho)_0 \langle v^2 \rangle} = \frac{\left\langle i \frac{\partial v}{\partial x} v \right\rangle}{\langle v^2 \rangle}. \quad (\text{A10})$$

For waves with a significant standing component, information about their position in relation to the stack can be represented by a parameter α , with

$$\alpha k_j^2 \equiv \frac{\left\langle \left(\frac{\partial v}{\partial x} \right)^2 \right\rangle}{\langle v^2 \rangle}. \quad (\text{A11})$$

Equation (A8) can then be grouped to read

$$\begin{aligned} \frac{\partial}{\partial x} \left\{ \left[\frac{1}{\Lambda} + \delta(x) \right] \frac{\partial T_0}{\partial x} - k_j \left[\gamma^2 - (\gamma-1)\sigma'(x) \right] T_0 \right\} \\ = (\gamma-1) k_j \left[2\alpha k_j \delta(x) T_0 - \sigma'(x) \frac{\partial T_0}{\partial x} \right]. \end{aligned} \quad (\text{A12})$$

Solutions to the homogeneous equation, obtained by setting the left-hand side equal to zero, actually contain everything interesting about Eq. (A12). This can be seen by defining

rescaled boundary layer functions $\tilde{\sigma} \equiv \sigma' e^{\pm \alpha k_j \sqrt{\gamma} \delta_\kappa (\sigma' + \delta)}$ and $\tilde{\delta} \equiv \delta e^{\pm (\gamma-1) k_j \sqrt{\gamma} \delta_\kappa (\sigma' + \delta)}$. From the definitions (A7), it follows that $\partial \sigma' / \partial x = \mp (\sigma' + \delta) / \sqrt{\gamma} \delta_\kappa$ and $\partial \delta / \partial x = \pm (\sigma' - \delta) / \sqrt{\gamma} \delta_\kappa$, respectively, at x_H and x_C , so Eq. (A12) can be written

$$\frac{\partial}{\partial x} \left\{ \left[\frac{1}{\Lambda} + \tilde{\delta}(x) \right] \frac{\partial T_0}{\partial x} - k_j [\gamma^2 - (\gamma-1) \tilde{\sigma}(x)] T_0 \right\} \approx 0. \quad (\text{A13})$$

Here the approximately equals sign indicates small modifications in the shape of the terms that have been kept, *only* in the middle of the boundary layer where the particular shapes of σ' and δ have no effect on the qualitative form or scaling of the solution. Because the changes are by scale factors and not constant offsets, they will not modify the asymptotic relations between heat current and sound power derived below and the difference between Eq. (A13) and the homogeneous part of Eq. (A12) will not be visible in results at the orders of $\gamma-1$ and $k_j \delta_\kappa$ kept. (Therefore δ and σ' will be retained in the notation.)

From the energy conservation relation (6) and the form (7) for the heat flux, suppressing terms of order v^3 , the total mean energy current through the region without sources is given to second order by

$$\begin{aligned} & \frac{\gamma-1}{(\tilde{\kappa}\rho)_0 \Lambda} \left\langle \frac{\gamma \rho v T}{\gamma-1} - \frac{\tilde{\kappa} \rho}{\gamma-1} \frac{\partial T}{\partial x} \right\rangle_{\text{no source}} \\ &= k_j \gamma^2 T_0 - \frac{1}{\Lambda} \frac{\partial T_0}{\partial x} \quad (T_1 \text{ adiabatic}) \\ &= k_j \gamma T_0 - \frac{1}{\Lambda} \frac{\partial T_0}{\partial x} \quad (T_1 \equiv 0). \end{aligned} \quad (\text{A14})$$

These are the two forms appearing in Eq. (A13) on either side of the boundary region δ , where σ' takes values 0 and 1, respectively (working to linear order in $\gamma-1$). This verifies that energy conservation is maintained within the mean-field approximation and shows that δ defines the transition region between adiabatic and isothermal sound.

The solution of Eq. (A13) is by means of an integrating factor. Defining a dilated coordinate

$$dz \equiv \frac{1}{1 + \Lambda \tilde{\delta}(x)} dx, \quad z(x_H) \equiv 0, \quad z(x_C) \equiv z_C, \quad (\text{A15})$$

and the argument of the integrating factor

$$\xi(z) \equiv \Lambda k_j \int_0^z dz' [\gamma^2 - (\gamma-1) \sigma'], \quad (\text{A16})$$

the exact solution to Eq. (A13) is given by

$$\begin{aligned} T_0(z) &= T_H \frac{\int_z^{z_C} dz' e^{-[\xi(z') - \xi(z)]}}{\int_0^{z_C} dz' e^{-\xi(z')}} \\ &+ T_C e^{-[\xi(z_C) - \xi(z)]} \frac{\int_0^z dz' e^{-\xi(z')}}{\int_0^{z_C} dz' e^{-\xi(z')}}. \end{aligned} \quad (\text{A17})$$

The imaginary part δ of the boundary layer, rather than being the working term as in the thermoacoustic cycle, is a parasitic loss region. Its effect can be seen by examining the leading term in the exact solution (A17) at large sound level. In the midadiabatic return path of the annulus for large $\Lambda k_j L$, the second term in Eq. (A17) is exponentially suppressed and the first term approaches the constant value

$$T_0(z) \sim T_H \exp \left(-(\gamma-1) k_j \int_0^{L/2} \frac{dx \sigma'(x)}{\frac{1}{\Lambda} + \delta(x)} \right). \quad (\text{A18})$$

The temperature in the adiabat is thus determined by convection of whatever emerges at the hot end of the source region. Explicit integration, using the forms (A7) for σ' and δ , gives

$$\begin{aligned} & \frac{1}{\sqrt{\gamma} \delta_\kappa} \int_0^{L/2} \frac{dx \sigma'(x)}{\frac{1}{\Lambda} + \delta(x)} \approx \frac{\Lambda}{2} \quad (\Lambda \lesssim 1) \\ & \approx \ln \Lambda \quad (\Lambda \gg 1) \end{aligned} \quad (\text{A19})$$

and leads to a scaling relation for T_0 of the form

$$\begin{aligned} \frac{T_0(z)}{T_H} &\sim e^{-(\gamma-1) k_j \sqrt{\gamma} \delta_\kappa (\Lambda/2)} \quad (\Lambda \lesssim 1) \\ &\sim \Lambda^{-(\gamma-1) k_j \sqrt{\gamma} \delta_\kappa} \quad (\Lambda \gg 1). \end{aligned} \quad (\text{A20})$$

For rms gas displacement less than δ_κ , the gas emerges at nearly the temperature of the hot exchanger. However, for larger displacements, at which isothermal sound is transported out of conductive contact with the strongly coupled source, energy must be drawn from the background T_0 to provide the fluctuating temperature component of the adiabatic sound. This cools the gas below the temperature of the hot exchanger. The transport relations will show that mechanical work is drawn from the sound wave to do this, so the boundary layer in effect implements a refrigeration cycle that consumes part of the gain produced by the stack. Examples of the solution (A17) are shown in Fig. 4.

The action of the stack as a Stirling regenerator can be checked by evaluating the comoving entropy change, which in the stack interior is given by

$$\left\langle \rho T \frac{ds}{dt} \right\rangle = \frac{1}{\gamma-1} \langle \rho_1 v \rangle \frac{\partial T_0}{\partial x} = - \frac{\partial}{\partial x} j_{\text{reg}}. \quad (\text{A21})$$

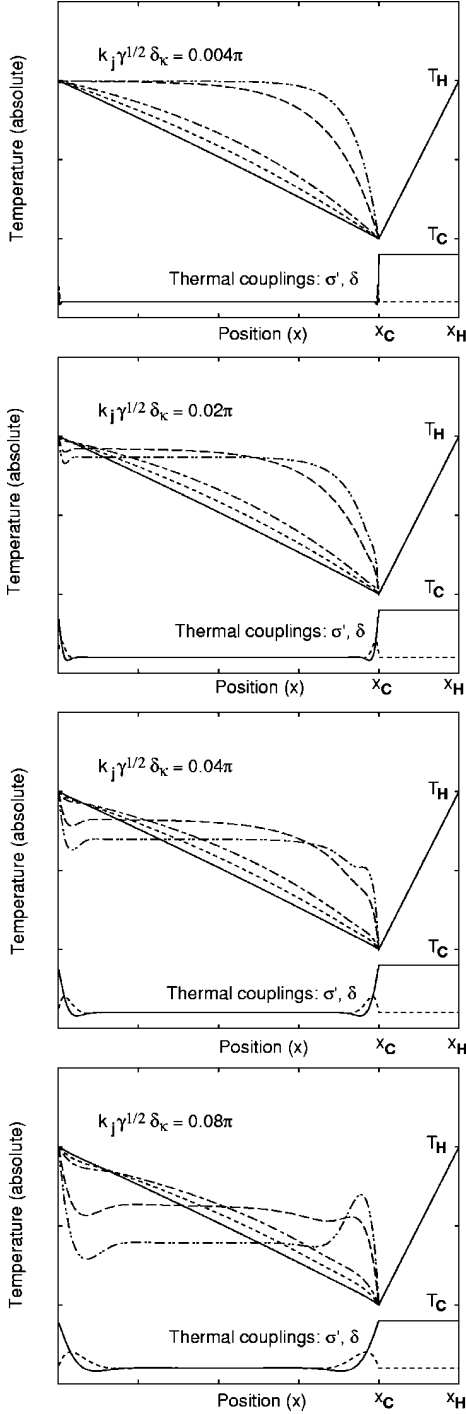


FIG. 4. Forms of the background temperature profile for varying wave number and sound intensity. Wavelength is one cycle in the periodic domain in all frames; the boundary layer width can be seen from graphs of σ' and δ . The sequence of Λ values is $\Lambda = \{0.01, 0.05, 0.1, 0.5, 1.0\}$, in order from the solid line to the most distorted profile. Source temperatures are normalized, with $(T_H - T_C)/T_C = 0.1$.

Adding this contribution to the convected enthalpy term gives

$$\left\langle \frac{\rho v T}{\gamma - 1} + j_{\text{reg}} \right\rangle_{\text{stack}} = 0. \quad (\text{A22})$$

Thus the strongly coupled regenerator permits no enthalpy flow downstream with the gas, as desired. As noted by Ceperley [8], heat must flow in the stack, in the direction opposite the wave transport. This can be seen by evaluating the work flux current

$$j_{\text{work}} = \langle \rho v T \rangle = \langle \rho_1 v \rangle T_0. \quad (\text{A23})$$

j_{work} is not conserved, so energy conservation in the stack requires a *backward* heat flux current to power the pumping of the gas.

The discontinuity of the heat flux current at the stack ends gives the net heat flow from the sources because the work flux is continuous through those points. The dependence of the heat flow \dot{Q} into the cold reservoir (out of the engine) on the state of the engine is

$$\dot{Q}_{\text{out},C} = \frac{1}{\gamma - 1} (\tilde{\kappa}\rho)_0 k_j \Lambda \left\{ \left[\gamma^2 T_0 - \frac{1}{k_j \Lambda} \frac{\partial T_0}{\partial x} \right]_{\text{cons}} - (\gamma - 1) T_C \right\}. \quad (\text{A24})$$

The total energy current may be evaluated in the midadiabatic range, where T_0 takes a simple form, and conservation then ensures that this has the same value at the stack edges. In the scaling regimes considered above, this current behaves as

$$\begin{aligned} & \frac{\gamma - 1}{(\tilde{\kappa}\rho)_0 k_j \gamma^2 \Lambda} \dot{Q}_{\text{out},C} \rightarrow e^{-(\gamma - 1)k_j \sqrt{\gamma} \delta_\kappa (\Lambda/2)} T_H \\ & - \frac{\gamma - 1}{\gamma^2} T_C \quad (\Lambda \leq 1) \rightarrow \Lambda^{-(\gamma - 1)k_j \sqrt{\gamma} \delta_\kappa} T_H \\ & - \frac{\gamma - 1}{\gamma^2} T_C \quad (\Lambda \geq 1). \end{aligned} \quad (\text{A25})$$

Meanwhile, the work flux undergoes a very complicated behavior in passage through the cold boundary layer, the stack, and the hot boundary layer. The loss of transported pressure through the latter indicates that work is being done to pump heat in the hot boundary and the complementary result is a dumping of energy in the cold boundary layer because the temperature oscillations of the adiabatic sound are not permitted to pass through the stack. The work difference that actually drives an increase of sound in the engine is not the naive value $\langle \rho_1 v \rangle (T_H - T_C)$, which corresponds to the idealized gain in Ref. [7], but rather that obtained interior to the boundary layers, where the gas is adiabatic

$$\Delta j_{\text{work}} \approx \gamma \langle \rho_1 v \rangle [T_0(x_H + \sim \sqrt{\gamma} \delta_\kappa) - T_0(x_C - \sim \sqrt{\gamma} \delta_\kappa)]. \quad (\text{A26})$$

As can be seen in Fig. 4, this difference can be much smaller than the value at the stack ends. The stability analysis for sound modes in the background of the mean temperature

field (A17) will provide an explicit definition for the effective positions at which T_0 should be evaluated in Eq. (A26).

APPENDIX B: LINEAR STABILITY AND QUALITY

The coordinate transformation method for extracting eigenvalues and eigenvectors in this section, which recovers the short-stack gain result at zero dissipation [8], may be seen as an explicit prescription for self-consistently integrating out oscillator fluctuations to produce the Ginzburg-Landau potential for mode amplitudes of Sec. IV.

The velocity modes and frequencies may be found in an arbitrary thermal background because the coordinates for one-dimensional motion can be dilated or contracted to compensate for the effects of nonuniform temperature, after which the eigenmodes appear as uniform traveling waves in the new coordinates.

The expansion for the heat term (A1) is substituted into the equation of motion (9), giving, at linear order in v ,

$$\frac{d^2v}{dt^2} = \gamma P_0 \frac{\partial}{\partial m} \left\{ \frac{\partial v}{\partial x} \left(1 - \frac{\gamma-1}{\gamma} (\sigma' - i\delta) \right) - \frac{1}{\gamma T_0} \frac{\partial T_0}{\partial x} (\sigma' - i\delta) v \right\}. \quad (\text{B1})$$

This can be cast as an eigenvalue problem using the inner product defined by integration over the periodic domain

$$- \oint dx \frac{1}{\gamma T_0} v^* \frac{d^2v}{dt^2} = \oint dx \frac{\partial v^*}{\partial x} \left\{ \left(1 - \frac{\gamma-1}{\gamma} (\sigma' - i\delta) \right) \frac{\partial v}{\partial x} - \frac{1}{\gamma T_0} \frac{\partial T_0}{\partial x} (\sigma' - i\delta) v \right\} \quad (\text{B2})$$

(where an asterisk denotes complex conjugation). The case $\gamma-1 \rightarrow 0$ will be considered first because it affords a useful simplification of the kinetic term. Defining

$$\varphi_0^* \equiv \frac{1}{\gamma T_0} \frac{\partial T_0}{\partial x} (\sigma' - i\delta), \quad (\text{B3})$$

one looks for solutions to the equation

$$\lambda^* v^* = - \frac{\partial^2 v^*}{\partial x^2} - \varphi_0^* \frac{\partial v^*}{\partial x}, \quad (\text{B4})$$

from which Eq. (B2) gives

$$\frac{\omega^2}{c^2} \equiv \frac{\omega^2 \oint \frac{dx}{\gamma T_0} v^* v}{\oint dx v^* v} = \lambda^*. \quad (\text{B5})$$

Diagonalization of Hermitian operators is easier than for general matrices, so it is useful to consider the *pair* of eigenvalue relations that can be obtained from Eq. (B4) for the same solution v ,

$$\lambda^* \oint dx v^* v = - \oint dx \left(\frac{\partial^2 v^*}{\partial x^2} + \varphi_0^* \frac{\partial v^*}{\partial x} \right) v,$$

$$\lambda^* \lambda \oint dx v^* v = \oint dx \left(\frac{\partial^2 v^*}{\partial x^2} + \varphi_0^* \frac{\partial v^*}{\partial x} \right) \times \left(\frac{\partial^2 v}{\partial x^2} + \varphi_0 \frac{\partial v}{\partial x} \right). \quad (\text{B6})$$

The second equation will be used to identify a diagonalization algorithm based on a sequence of coordinate transformations. First, define a zeroth-order iteration variable $w_0 \equiv \partial v / \partial x$, reducing unnecessary derivatives. Equation (B6) becomes

$$\lambda^* \oint dx v^* v = - \oint dx \left(\frac{\partial w_0^*}{\partial x} + \varphi_0^* w_0^* \right) v,$$

$$\lambda^* \lambda \oint dx v^* v = \oint dx \left(\frac{\partial w_0^*}{\partial x} + \varphi_0^* w_0^* \right) \times \left(\frac{\partial w_0}{\partial x} + \varphi_0 w_0 \right). \quad (\text{B7})$$

Next define a dummy coordinate $y_0 \equiv x$ to standardize notation for an iterated sequence. Choosing an arbitrary but fixed physical location to take value 0 in all the succeeding coordinate systems, make the definitions, $\forall i \geq 0$,

$$\bar{\varphi}_i \equiv \frac{1}{\oint dy_i} \oint dy_i \varphi_i,$$

$$f_{i+1} \equiv \int_0^{y_i} dy_i' (\varphi_i - \bar{\varphi}_i),$$

$$w_i \equiv e^{-f_{i+1}} w_{i+1}, \quad (\text{B8})$$

$$dy_i \equiv dy_{i+1} e^{-2 \operatorname{Re}(f_{i+1})},$$

$$\varphi_{i+1} \equiv \bar{\varphi}_i e^{-2 \operatorname{Re}(f_{i+1})}.$$

After performing N such changes of variable, Eq. (B7) takes the form

$$\lambda^* \oint dx v^* v = - \oint dy_N \left(\frac{\partial w_N^*}{\partial y_N} + \varphi_N^* w_N^* \right) \times \left(\prod_{i=1}^N e^{-f_i v} \right),$$

$$\lambda^* \lambda \oint dx v^* v = \oint dy_N \left(\frac{\partial w_N^*}{\partial y_N} + \varphi_N^* w_N^* \right) \times \left(\frac{\partial w_N}{\partial y_N} + \varphi_N w_N \right). \quad (\text{B9})$$

The main points of the construction are these. Each independent eigenpair (v, λ) maps to an independent solution w_N at any given order N . Each independent value of $\lambda^* \lambda$ does the same. The Hermitian operator can be diagonalized in any coordinates that are convenient and the resulting diagonalization must be unique as long as the values of $\lambda^* \lambda$ are unique (which will be seen to hold). The motivation for the sequence of definitions (B8) is that successive coordinate transformations progressively strip higher harmonic content from the oscillatory functions φ_i . For instance, with σ' a simple step, φ_0 has discontinuous values, φ_1 only discontinuous first derivatives, etc. Explicit consideration of the coefficients $\varphi^{(j)}$ of individual harmonics in an expansion $\varphi_0 = \sum_j \varphi^{(j)} e^{2\pi j x i/L}$ shows that these decay with each iteration roughly as $(\bar{\varphi}_N L / j \pi)^N$. The requirement that $(\bar{\varphi}_N L / j \pi)^N \rightarrow 0$ is nothing more than a stipulation that the pipe as an acoustic resonator controls the leading form of the sound modes and not the perturbation introduced by φ_0 . Thus at large N , φ_N converge to a constant. In that limit, the diagonalization is elementary, though the relation to v in the original coordinates no longer is. Therefore, define

$$y \equiv \lim_{N \rightarrow \infty} y_N,$$

$$\bar{\varphi} \equiv \lim_{N \rightarrow \infty} \varphi_N, \quad (\text{B10})$$

$$e^{-f} \equiv \lim_{N \rightarrow \infty} \prod_{i=1}^N e^{-f_i}.$$

In terms of these, the eigenvalue λ may be written using Eq. (B9) as

$$\lambda = (k^2 + ik\bar{\varphi}) \frac{\oint dy}{\oint dy e^{iky} \left(e^{-f} \frac{v}{v_R} \right)}, \quad (\text{B11})$$

where k is any wave number allowed in the periodic domain of y , v_R is an arbitrary reference scale for velocities, and v is the solution corresponding to $w = -ike^{-iky} v_R$ under the coordinate transformation. The denominator of Eq. (B11) can be evaluated entirely in terms of f and k as

$$\frac{1}{v_R} \oint dy e^{iky} (e^{-f} v) = \oint dy e^{-f(y)} \int_y^0 du (ik) e^{iku} e^{-f(y-u)} \times e^{-2 \operatorname{Re}[f(y-u)]}. \quad (\text{B12})$$

The way this solution works can be seen by considering the case of an indefinitely extended stack, $\varphi_0 = \text{const}$, equivalent to the idealized analysis of Ref. [7]. This is an ‘‘Escherian’’ temperature profile, increasing uniformly at all points in a periodic domain (hence unphysical), for which $\varphi_0 = \bar{\varphi}$, $f_i = 0 \forall i$, $dy = dx$, $-ik v = w$, and $\oint dy e^{iky} (e^{-f} v) = \oint dy e^{iku} |_{y=0} = \oint dy$. Therefore,

$$\lambda^* = (k^2 - ik\varphi_0^*) = \omega^2 \frac{\oint dx \frac{1}{\gamma T_0}}{\oint dx} = \frac{\omega^2}{c^2}. \quad (\text{B13})$$

The real parts of mode eigenvalues are not affected, while the traveling wave with current in the same direction as the temperature gradient has a negative imaginary part and is exponentially growing, and its conjugate is damped with the same time constant.

In physically meaningful cases where $\varphi_0 \neq \text{const}$, the leading-order approximation to $\bar{\varphi}$ is still given by taking the average value of Eq. (B3) to yield

$$\operatorname{Re} \left(\frac{\omega^2}{c^2} \right) \approx k^2 - \frac{k}{L} \oint dx \frac{1}{\gamma T_0} \frac{\partial T_0}{\partial x} \delta, \quad (\text{B14})$$

$$\operatorname{Im} \left(\frac{\omega^2}{c^2} \right) \approx \frac{-k}{L} \oint dx \frac{1}{\gamma T_0} \frac{\partial T_0}{\partial x} \sigma'.$$

These values are then corrected by the perturbations to k , $\bar{\varphi}$, and the denominator in Eq. (B11) from higher-order harmonic content of f .

Including working terms proportional to $\gamma - 1$ in Eq. (B1) does two things. If the modification $i\delta(\gamma - 1)/\gamma$ to the kinetic term is treated as a perturbation, the remaining corrections to Eq. (B2) can be absorbed in a redefined coordinate $dx \equiv dx' [1 - \sigma'(\gamma - 1)/\gamma]$. Setting $y_0 = x'$, the iterative reduction is performed as before. While the form of the leading-order approximation (B14) for ω^2 is the same, the temperature profile is modified by the boundary layer effects described in Appendix A. In particular, the form

$$\operatorname{Im} \left(\frac{\omega^2}{c^2} \right) \approx \frac{-k}{L} \oint dx \frac{1}{\gamma T_0} \frac{\partial T_0}{\partial x} \sigma'$$

$$\equiv \frac{-k}{L} [\ln T_0(x_H + \sim \sqrt{\gamma} \delta_\kappa) - \ln T_0(x_C - \sim \sqrt{\gamma} \delta_\kappa)] \quad (\text{B15})$$

provides the definition of the effective temperature difference appearing in Eq. (A26) in terms of the frequency-dependent coupling strength σ' . For large Λ or higher modes (large $k_j L$), the thermal impedance mismatch can re-

duce the effective Δj_{work} driving the engine to zero at finite transport because the temperature difference at the ends of the boundary layers in Fig. 4 goes to zero.

When the kinetic perturbation $i\delta(\gamma-1)/\gamma$ is added, its first-order effect on a solution with $k \approx k_j$, as defined in Eq. (A10), is to induce a *positive* imaginary shift

$$\begin{aligned} \frac{\omega^2}{c^2} &\rightarrow \frac{\omega^2}{c^2} + i \frac{\gamma-1}{\gamma} \frac{\oint dx \frac{\partial v^*}{\partial x} \frac{\partial v}{\partial x} \delta(x)}{\oint dx v^* v} \\ &\approx \frac{\omega^2}{c^2} + i k_j^2 \alpha \frac{\gamma-1}{\sqrt{\gamma}} \frac{\delta_\kappa}{L}, \end{aligned} \quad (\text{B16})$$

independent of transport and determined solely by the velocity gradients in the boundary layers. Taking the square root

of Eq. (B14), also for $k \approx k_j$, gives the leading dependence of the real and imaginary wave numbers on the stack temperature difference when $\gamma-1 \rightarrow 0$:

$$\begin{aligned} \text{Re}\left(\frac{\omega}{c}\right) &\approx |k_j| \mp \frac{1}{2L} \oint dx \frac{1}{\gamma T_0} \frac{\partial T_0}{\partial x} \delta, \\ \text{Im}\left(\frac{\omega}{c}\right) &\approx \mp \frac{1}{2L} \oint dx \frac{1}{\gamma T_0} \frac{\partial T_0}{\partial x} \sigma'. \end{aligned} \quad (\text{B17})$$

The expressions for the reversible and irreversible eigenfrequencies may now be inserted into the definition (11) of the quality factor to show that its inverse is linear in ΔT in all cases and that the offset term giving a nonzero T_{crit} comes entirely from irreversible effects and vanishes in the reversible limit.

-
- [1] N. Rott, *Z. Angew. Math. Phys.* **26**, 43 (1975).
- [2] N. Rott, *Z. Angew. Math. Phys.* **24**, 54 (1973); *Adv. Appl. Mech.* **20**, 135 (1980).
- [3] J. Wheatley, T. Hofter, G. W. Swift, and A. Migliori, *J. Acoust. Soc. Am.* **71**, 153 (1983).
- [4] G. W. Swift, *J. Acoust. Soc. Am.* **84**, 1145 (1988).
- [5] A. A. Atchley, H. E. Bass, T. J. Hofter, and H.-T. Lin, *J. Acoust. Soc. Am.* **91**, 734 (1992).
- [6] A. A. Atchley, *J. Acoust. Soc. Am.* **95**, 1661 (1994).
- [7] P. H. Ceperley, *J. Acoust. Soc. Am.* **66**, 1508 (1979).
- [8] P. H. Ceperley, *J. Acoust. Soc. Am.* **72**, 1688 (1982); **77**, 1239 (1985); **85**, S48(A) (1989); U. S. Patent No. 4355517 (26 October 1982).
- [9] R. Raspet, H. E. Bass, and J. Kordomenos, *J. Acoust. Soc. Am.* **94**, 2232 (1993); see also R. Raspet, *ibid.* **100**, 673(E) (1996) for the appropriate scope of this work. The importance of longitudinal conduction along the stack in implementing the Stirling regenerator is discussed in Appendix A.
- [10] H.-T. Lin and A. Atchley, *J. Acoust. Soc. Am.* **100**, 2646(A) (1996).
- [11] See Ref. [4], Fig. 4, p. 1148.
- [12] K. G. Wilson and J. Kogut, *Phys. Rep., Phys. Lett.* **12C**, 75–200 (1974), Introduction, Sec. 2.1, pp. 87–89.
- [13] See Ref. [12], Introduction, pp. 78–86.
- [14] This has been attempted, unsuccessfully, in the course of other work, but not pursued; A. Atchley (private communication).
- [15] S. Coleman, *Aspects of Symmetry* (Cambridge University Press, New York, 1985), Chap. 5, pp. 113–184; S. Weinberg, *The Quantum Theory of Fields* (Cambridge University Press, Cambridge, 1996), Vol. II, Chap. 19.
- [16] This association may not be intrinsic though. For a counterexample, in the case of flow away from an unstable critical point, see the treatment of critical localization in A. J. McKane and M. Stone, *Ann. Phys. (N.Y.)* **131**, 36 (1981).
- [17] S. Coleman, *Aspects of Symmetry* (Ref. [15]), p. 118, and references therein.
- [18] S.-K. Ma, *Modern Theory of Critical Phenomena* (Benjamin/Cummings, London, 1976), p. 67.
- [19] L. E. Reichl, *A Modern Course in Statistical Physics* (University of Texas Press, Austin, 1987), Chap. 17, pp. 623–654.
- [20] Enrico Fermi, *Thermodynamics* (Dover, New York, 1956).
- [21] Gerald D. Mahan, *Many-Particle Physics* (Plenum, New York, 1990), Chap. 3, pp. 133–238.
- [22] For definitions and properties see A. J. Organ, *Thermodynamics and Gas Dynamics of the Stirling Cycle Machine* (Cambridge University Press, New York, 1992), Chap. 5, pp. 76–92.
- [23] A traveling-wave engine capable of onset has not yet been built because the comparable width of viscous and thermal boundary layers in conventional stack engines creates flow losses greater than the stack gain. Due to the generically $O(1)$ value of the Prandtl number for gases, this is a serious problem, but is arguably a technical limitation of solid/gas plate stacks, which other regeneration methods may overcome.
- [24] This combination of assumptions is necessary to isolate the symmetries and conservation laws of a reversible limit. Though unrealistic for conventional engines, it is not inconsistent with the definition of the reversible cycle as a limiting behavior.
- [25] K. Huang, *Statistical Mechanics* (Wiley, New York, 1987), Sec. 6.4, pp. 136–138.
- [26] If the separation of scales between long-wavelength and short-wavelength modes is not wide, the notion of local corrections to the dynamical equations loses its meaning. In that case, more complex corrections to the correlation functions can be obtained by replacing the Matsubara diagram expansion with that of Keldysh: see E. M. Lifshitz and L. P. Pitaevsky, *Physical Kinetics* (Pergamon, New York, 1980), Chap. 10, pp. 391–412. The actions (2) and (5), however, are appropriate for this discussion.
- [27] See the review of Swift [4] for a more comprehensive list.
- [28] J. R. Olson and G. W. Swift, *J. Acoust. Soc. Am.* **95**, 1405 (1994).
- [29] The factor of $\sqrt{\gamma}$ relating the boundary layer thickness in this calculation to δ_κ is an artifact of the choice to expand in ρ and v instead of the p and u of Ref. [4]. The difference term of order $(\gamma-1)\delta_\kappa$ is comparable to bulk conduction terms that are ignored.